Kund, anläggning	Datum	Författare
3B, Ungern	2023-03-02	
Dokumenttyp	Projekt nr.	Dok.id.
Testrapport	2219-	ZZ00U01

Catalytic filter for removal of hydrocarbons in RDF pyrolysis vapors: Tests performed in a pilot pyrolysis plant at 3B, Zalaegerszeg, Hungary.

Christer Rosén, Peter Blomdahl, Klas Engvall

1. Introduction

The company 3B, located in Zalaegerszeg, Hungary, aims at developing a pyrolysis technology for utilizing refused derived fuel (RDF) feedstocks as a for producing heat and power. At present the pilot plant gas cleaning process is suitable for combustion of the pyrolysis vapors in a combustor for producing heat. The plan is to develop a gas cleaning process to enable a use of the energy rich gas in a gas engine to produce power. Major issues are the too high content of particles and biooil compounds in the pyrolysis vapors, which need to be removed before the gas enters the gas engine. The report presents results from test aimed at investigating the performance of a catalytic filter in terms of reducing the biooil content in the gas. The tests were performed onsite at 3B's pilot plant pyrolyzer in in November 22-23, 2022.

2. Short background pyrolysis

Pyrolysis of biomass can be divided into conventional or slow pyrolysis, intermediate pyrolysis and fast/flash pyrolysis (Table 1). This somewhat arbitrary classification is related to the influence of heating rate on product distribution. Generally, lower process temperature and long vapor residence time decrease the gas and oil yield, whereas high temperature and long residence time increase the gas and oil yield. Moderate temperature and short vapor residence time favors production of liquids. Fast pyrolysis is of particular interest due to high yields of liquid (bio-crude) which can further be used in variety of applications.

Table 1 Temperature ranges and heating rates for slow, intermediate, and fast pyrolysis[1]

Type of pyrolysis	Slow	Intermediate	Fast
Temperature (K)	550 - 950	500 - 650	850 – 1250
Heating rate (K/s)	0.1 – 1.0	1.0 - 10	10 – 200

The biomass pyrolysis mechanism is not well understood. Nevertheless, details of reaction involved in biomass pyrolysis pathways for cellulose, hemicellulose, and lignin are available in several reviews and studies[2]. A general reaction formula for biomass would be:

[1] Demirbas A, Arin G. An Overview of Biomass Pyrolysis. Energy Sources 2002;24:471-482

[2] Le Brech Y, Jia L, Cissé S, Mauviel G, Brosse N, Dufour A. Mechanisms of biomass pyrolysis studied by combining a fixed bed reactor with advanced gas analysis. J Anal Appl Pyrolysis 2016;117:334-346

Kontor	Kontakt	Kontakt	Org nr / VAT No
SiteConcept AB Gäddvägen 1 SE-761 42 Norrtälje Sweden	Anders Toll +46 70 209 42 19 anders.toll@siteconcept.se	Peter Blomdahl +46 70 380 23 63 peter.blomdahl@siteconcept.se	559163-5882 SE559163588201

Biomass + heat → Biooil + biochar + CO + CO_2 + H_2 + H_2O + CH_4 + C_2-C_6 hydrocarbons + inorganics

The formation process of biooil or condensable organics and their maturing is shown in Figure 1. The figure shows the transition as a function of process temperature from primary products to phenolic compounds to aromatic hydrocarbons. Therefore, the composition of pyrolysis oil is very complex and can contain up to around 300 organic compounds depending on temperature, heating rate and feedstock.

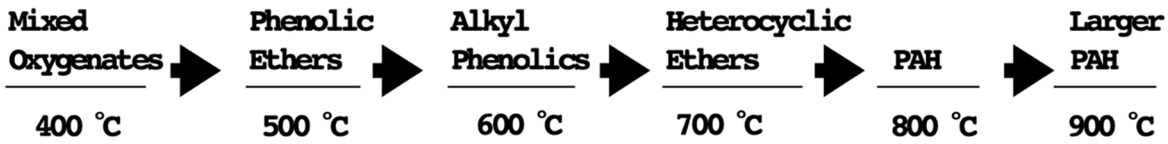

Figure 1 Tar (condensable organic compounds) maturation scheme proposed by Elliot[3]

A conceptual relationship between the yield of "condensable organics" and the reaction temperature is shown in Figure 2.

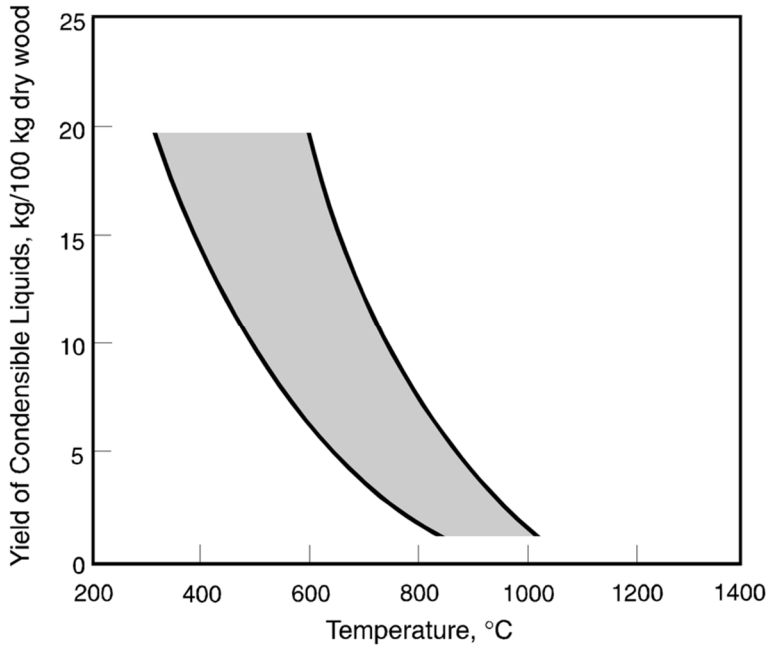

Figure 2 Condensable organics oil yield as a function of temperature exposure for wood by Baker at al[4]

The catalytic decomposition of the hydrocarbons (aromatics, phenolics, etc) are very complex as displayed in Figure 3, an example to provide a hint of a suggested reaction mechanism of a major stable compound naphthalene present in the pyrolysis vapor.

[3] Elliott, D.C. 1988. "Relation of Reaction Time and Temperature to Chemical Composition of Pyrolysis Oils," ACS Symposium Series 376, Pyrolysis Oils from Biomass. Edited by E.J. Soltes and T.A. Milne. Denver, CO. April 1987.

[4] Baker, E.G.; Brown, M.D.; Elliott, D.C.; Mudge, L.K. 1988. "Characterization and Treatment of Tars from Biomass Gasifiers," Denver, CO: AIChE 1988 Summer National Meeting, pp. 1–11.

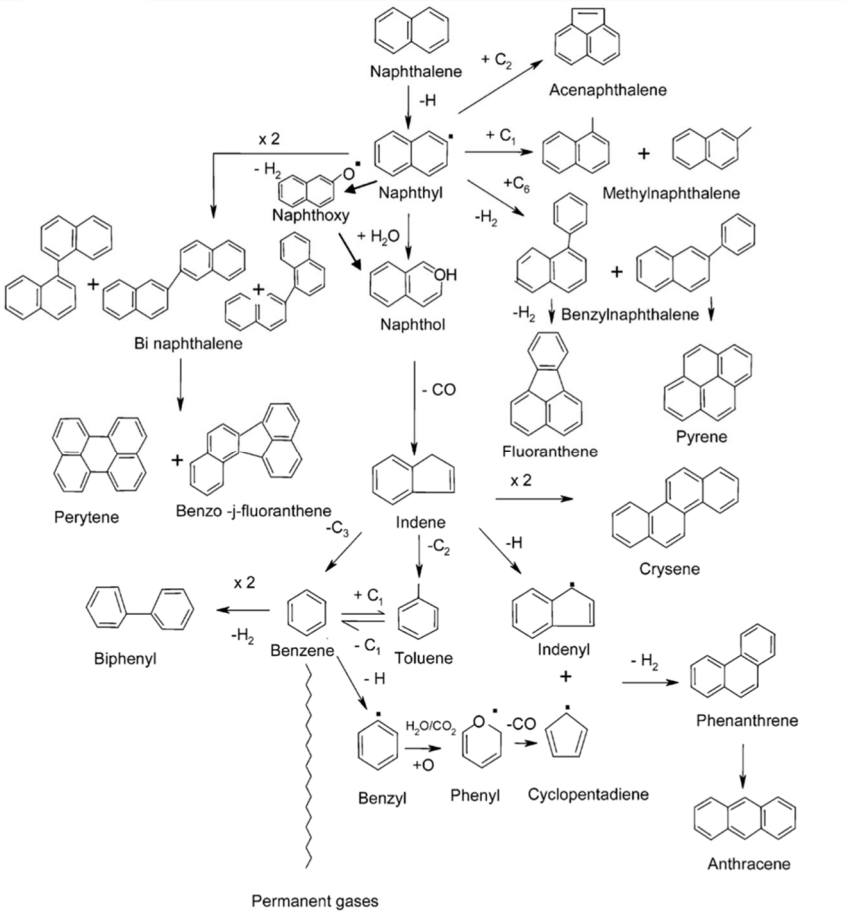

Figure 3 Reaction scheme for naphthalene decomposition.

3. Materials and methods

3.1. Fuel

The chemical composition and the heating values of the RDF used in the tests are listed in Table 2.

Table 2 RDF feedstock composition and heating values

Parameter	RDF 3B
Moisture [%]	5.39
Ash [% dry]	18.53
Carbon [% dry]	51.70
Oxygen [% dry]	21.65
Hydrogen [% dry]	7.00
Nitrogen [% dry]	1.12
Sulfur [% dry]	<0.2
HHV [MJ/kg wet]	22.14
HHV [MJ/kg dry]	23.40
LHV [MJ/kg wet]	20.58
LHV [MJ/kg dry]	21.90

HHV – High Heating Value
LHV – Low Heating Value

3.2. Filter elements used

The filter candles used in the experiments are provided by Tenmat Ltd. and are made of inorganically bonded granular minerals. The technical data are presented in Table 3. In case of the catalytic filter element, a nickel-based catalyst is deposited uniformly on the inner surface and pores of the filter candle. The even coating of the filter structure ensures a uniform contact time of the gaseous compounds over the whole length of the filter. A sketch of the catalytic filter element used in the experiments is shown in Figure 4.

Table 3 Technical data of the filter candles[5]

Density	450 kg/m^3
Pressure drop	35 mm H_2O at face velocity
Loss of ignition	6.3 % at 70 °C
Filtration efficiency	> 99.99 %
Typical air permeability	8 l/dm^2·min at 200 Pa
Filtration capability	< 1 Particle size (micron)
Emissions	< 1 mg/m^3
Temperature capability	≤ 1000 °C

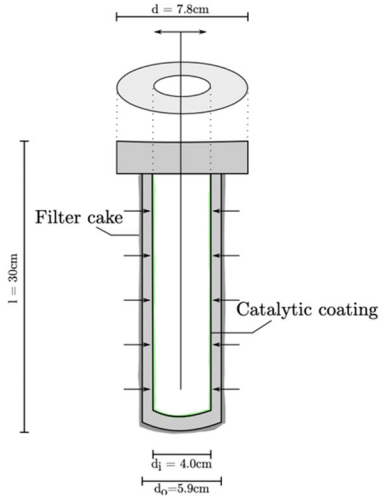

Figure 4 Sketch of the filter structure with a catalytic coating on the inner surface

3.3. Experimental setup

Figure 5 below shows the catalytic filter setup, used during the experimental test and how it is connected to a slipstream at the pyrolysis pilot plant at 3B. The ceramic candle filter is placed inside the reactor. The pyrolysis vapors from the slipstream are kept at 400 °C before it enters a pre-heater (750-800°C) followed by the filtration unit kept at 700°C. The filtered pyrolysis vapors leave the filtration unit at the top and is thereafter passing two coolers before the composition is analyzed with μ-GC. The flow rate of the dry gas is determined before the gas is exhausted. Ashes and other particulates that do not pass the filter are collected at the bottom in the ash bin. To be able to analyze the raw pyrolysis vapors, the gas may be diverted to a bypass line, equipped with a course particle filter, entering the same gas preparation steps before the GC and the flow meter. For a continuous control and accurate monitoring of the hot-gas filtration, temperature measurements are placed at specific positions of the experimental set-up. The pressure difference between inlet and outlet is monitored to obtain information

[5] Tenmat Ltd. Data sheet hot-gas filter. https://www.tenmat.com/high-temperature-materials/hot-gas-filtration/

about the pressure drop due to the possible formation of a filter cake or coking on the filter. Sampling points are installed at the in- and outlet to ensure representative tar sampling.

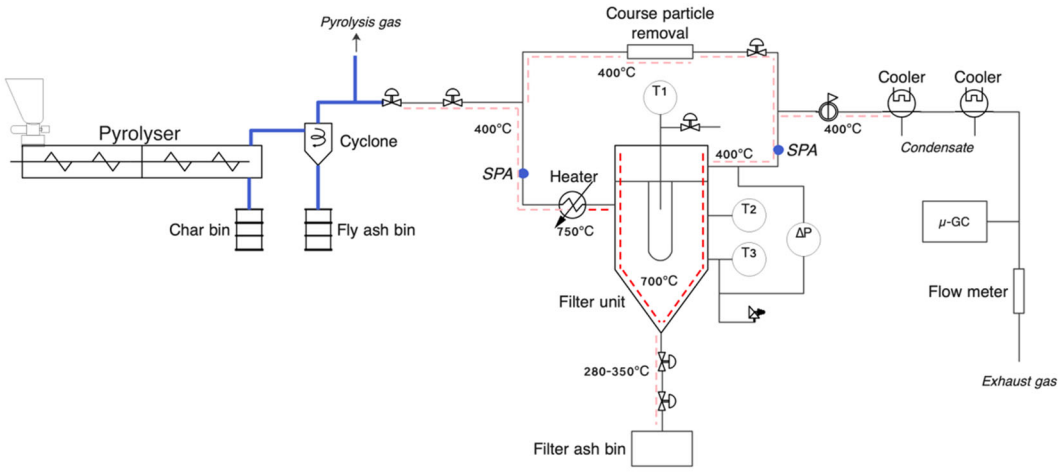

Figure 5 Catalytic filter test setup

3.4. Analysis of non-condensable gases and condensable organic compounds

The composition of the product gas stream is continuously analyzed and recorded using a micro gas-chromatograph (μ-GC). Bypassing the experimental unit with a side stream before the inlet enables an exact analysis of the untreated pyrolysis vapors. The device used for the analysis of the gas is a C2V-200 μ-GC, gas samples are taken every three minutes during the whole experimental runs. In parallel to the u-GC, a continuous a syngas gas analyzer Hubei Cubic-Ruiyi 3100P using IR & TCD technology. This gas analysis was performed by András Kállay at University of Miskolc, Hungary.

Samples of condensable organic compounds are taken before and after the filter reactor at stable operational conditions. The sampling points are shown in Figure 5. The composition and concentration of the tar compounds are analyzed by a solid-phase adsorption method (SPA). It is basically a method where the hydrocarbons are adsorbed on a solid phase sorbent using a syringe pump. For each sample 100 ml gas is sampled for 1 minute. The principle of SPA is based on trapping condensable organics (so-called tars) vapors and condensing them on a solid phase[6]. The samples are then analyzed by a gas-chromatograph and the conversion of tar products is determined. The method considers organics (aromatics 79-202 g/mol) and phenols (92-122 g/mol) and does not detect heavier hydrocarbons. Therefore, only part of all condensable organics can be analyzed with this method. However, qualitative changes in the content of condensable organics can provide with an understanding of changes in gas composition.

3.5. Ash content in solid samples

The ash content in the solid samples was determined according to the standard ISO18122:2015, where weighted solid samples in crucibles were heated up room temperature to 550 °C and thereafter again up to 830 °C. The samples were kept at the final temperature for 3 hours

[6] M.A. Svensson. Sampling and Analysis of Tars by Means of Photo Ionisation Detection and Solid Phase Micro Extraction. PhD thesis, 2013.

3.6. Operational parameters

The experiments were performed with the pyrolysis and filter unit operational conditions as specified in Table 4 and Table 5, respectively.

Table 4 Operational parameters the pyrolyzer

22-11-2022				
Start feeding	End feeding	Feeding rate (kg/h)	Pyrolysis temperature (°C)	Over pressure (mbar)
15:45	18:00	88 kg/h	600 – 700	10-12
23-11-2022				
Start feeding	End feeding	Feeding rate (kg/h)	Pyrolysis temperature (°C)	Over pressure (mbar)
11:46	13:38	93 kg/h	580 - 700	10-12

Table 5 Operational parameters the filter unit

22-11-2022							
Preheater (°C)	Gas in (°C)	Reactor top (°C)	Reactor bottom (°C)	Ash out (°C)	Bypass (°C)	dP filter (kPa)	Gas flow (NL/min dry)
800	750	700	580	325	400	4 - 13	ca 2
23-11-2022							
Preheater (°C)	Gas in (°C)	Reactor top (°C)	Reactor bottom (°C)	Ash out (°C)	Bypass	dP filter (kPa)	Gas flow (NL/min dry)
800	750	700	700	330	400	4 - 13	ca 2

Before starting the experiments using the pyrolysis vapors all temperatures and other settings were allowed to reach their set values, using a small gas stream of nitrogen through the system. The μ-GC and flow gas meter was also started well in advance of introducing the pyrolysis vapors. After the introducing the pyrolysis vapors to the filter reactor, the conditions were first allowed to stabilize before any SPA sampling was performed. Samples were collected before and after the filter reactor. To obtain the composition of non-condensable compounds in the raw pyrolysis vapors, the gas stream was diverted through the bypass to the gas cleaning system.

4. Results

4.1. General observations

4.1.1. Test with only filter November 22, 2022

The general observation is that the use of the filter was rather smooth and stable operation during the exposure to the pyrolysis vapors (16:07 – 17:07) as shown in Figure 8. Photos of the used filter is shown in Figure 6. The filter is completely black on the outside and partly on the inside of the element. The outside layer is hard and stable, and probably consists of char/ash particles mixed with condensable organic compounds, gluing the particles together. The inner black deposit is much thinner and probably mainly due to condensation of condensable organic compounds.

Figure 6 Photo of the candle filter after use November 22, 2022.

4.1.2. Test with catalytic filter November 23, 2022

The experiments operated rather smoothly during the exposure to the pyrolysis vapors (12:50 – 13:00), but of course with a variation in compound concentration due to the catalytically active filter, as shown in Figure 10. Photos of the used catalytic filter is shown in Figure 7. The filter is completely devoid of any deposits on the outside and the inside of the element. A potential reason could be a not completely airtight setup, caused by a leakage in the top flange of the filter reactor, which occurred when the catalytic filter element was installed. During cooling down of the reactor from 700 °C, the lowering of the temperature may have caused a negative pressure in the reactor and air slipping into the and oxidizing the carbon containing compounds on the filter element. On the inside the catalyst layer seems to be intact.

Figure 7 Photo of the catalytic filter after use November 23, 2022.

4.2. Gas composition

4.2.1. Non-condensable gases

From the analysis of the GC spectra, it is apparent that there are several peaks, corresponding to unknown compounds, which are not considered in the analysis. Therefore, the composition of non-condensable gases presented below do represent the true composition but only the relative difference between known compounds detected. Furthermore, the μ-GC result, regarding CO detecting, is a bit uncertain as the column in the μ-GC used for CO detection is sensitive to water in the sampled gas. A combination of very bad weather with heavy rain and a leaking gas sampling may explain the very low CO signal. Therefore, carbon balances were not carried out using the gas analysis obtained with the μ-GC but using the gas analysis performed by András Kállay at University of Miskolc.

Figure 8 shows the variation in non-condensable gases for the test using the candle filter November 22, 2022. The content of CO_2 is stable at 25 mol% during the period the pyrolysis vapors is passing through the candle filter, but when shifting the stream to the bypass a dramatic increase in the CO_2 content occurs. After switching back to the candle filter after back blowing the content decreases to its original level. Hydrogen starts at around 25 mol% and decreases

slowly to slightly lower than 20 mol % after an hour. This level continues also after the gas stream was shifted to the bypass, indicating that the decrease observed when the pyrolysis vapor passed through the filter possibly is due to changes in the pyrolysis process. Simultaneously as hydrogen decrease CH_4 and C_2H_4 is slowly increasing to the point the stream is shifted to the bypass. At this point the content of CH_4 is roughly unchanged but C_2H_4 decreases significantly mirroring the CH_4 curve. From this the candle filter evidently has a certain effect on the gas composition most likely by cracking of larger organic molecules. The CO content determined from the GC charts are very low compared to what has been reported in other studies. The reason for this is however not clear. Nevertheless, the observed CO signal follows the CO_2 content with an observable increase when the gas stream shifts to the bypass.

Figure 9 shows the gas analysis performed using the Hubei Cubic-Ruiyi 3100P gas analyzer, excluding N_2 and O_2. The gas analysis including N_2 and O_2 can be found in in Appendix 1. Note that axis for the sampling time is not the same as for the μ-GC and that nitrogen and oxygen is included in the analysis. From the analysis it is clear the gas composition differs from the on obtained by the μ-GC, exemplified by a higher CH_4 compared to CO_2 and a larger amount of CO in the gas. When shifting from raw pyrolysis gas to gas after filter there is large increase in CH_4, also in view of a slight increase of N_2, pointing at a potential intake of air in the sampling line. Interesting to note is also the slow increase in CH_4 and H_2, simultaneously as a decrease of C_nH_m in time (17:43 – 18:00) when measuring after the filter.

Figure 10 shows the variation in non-condensable gases for the test using the catalytic filter November 22, 2022. In case of using the catalytic filter there is a dramatic difference compared to when only the candle filter was exposed. For 25 – 30 minutes the content of CH_4 and H_2 is significantly higher 50 (at most) and 40 mol%, respectively, compared to CO_2 at 6-7 mol% and the remaining compounds below 1 mol%. After this initial period, the gas composition shifts to a similar one as for the candle filter element in Figure 8.

The gas analysis using the Hubei Cubic-Ruiyi 3100P gas analyzer, excluding N_2 and O_2, is shown in Figure 11. The gas analysis including N_2 and O_2 can be found in in Appendix 1. The pyrolysis vapors are passing through the catalytic filter during 12:05 - 12:22 where the catalyst displays a catalytic high activity. This is generally demonstrated by the high content of H_2 and CH_4 compared to the raw gas composition. The H_2 content in the gas starts to decline after around 11-12 minutes due to deactivation of the catalyst. Interesting to note is the nearly exact mirroring of the CH_4 curve. Also, CO and CO_2 follow similar tends as H_2 and CH_4. At a later stage (12:40 – 13:00) after pulsing the filter and pyrolysis gas through the catalytic filter, the gas composition is rather different compared to the previous period (12:05 - 12:22) with a very high content of CH_4. The other compounds are not too far from what is observed for the raw pyrolysis gas. Worth to note is the higher hydrogen content.

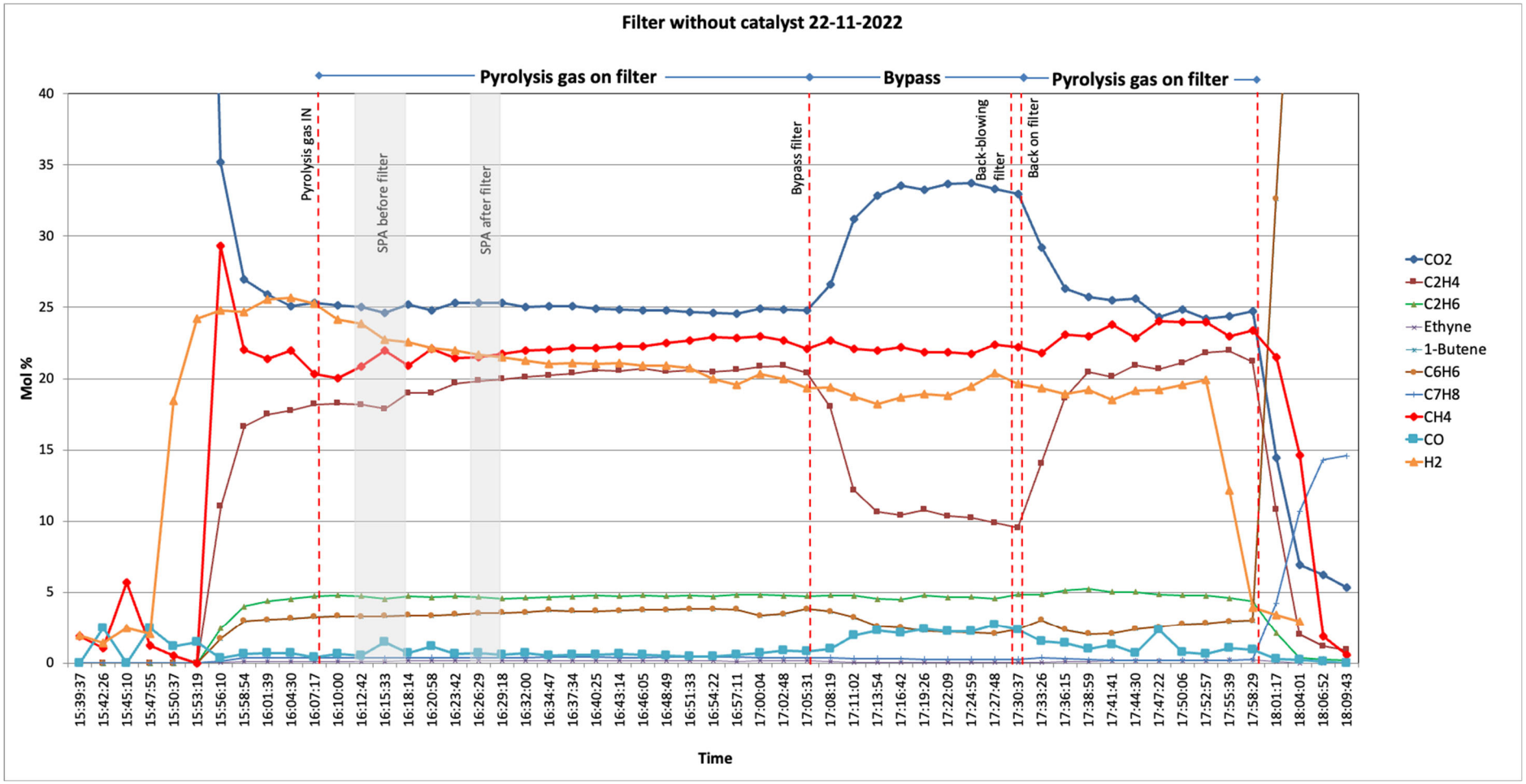

Figure 8 Composition of non-condensable gas components over time during the candle filter test November 22 measured with the µ-GC. The gas content is shown as oxygen and nitrogen free.

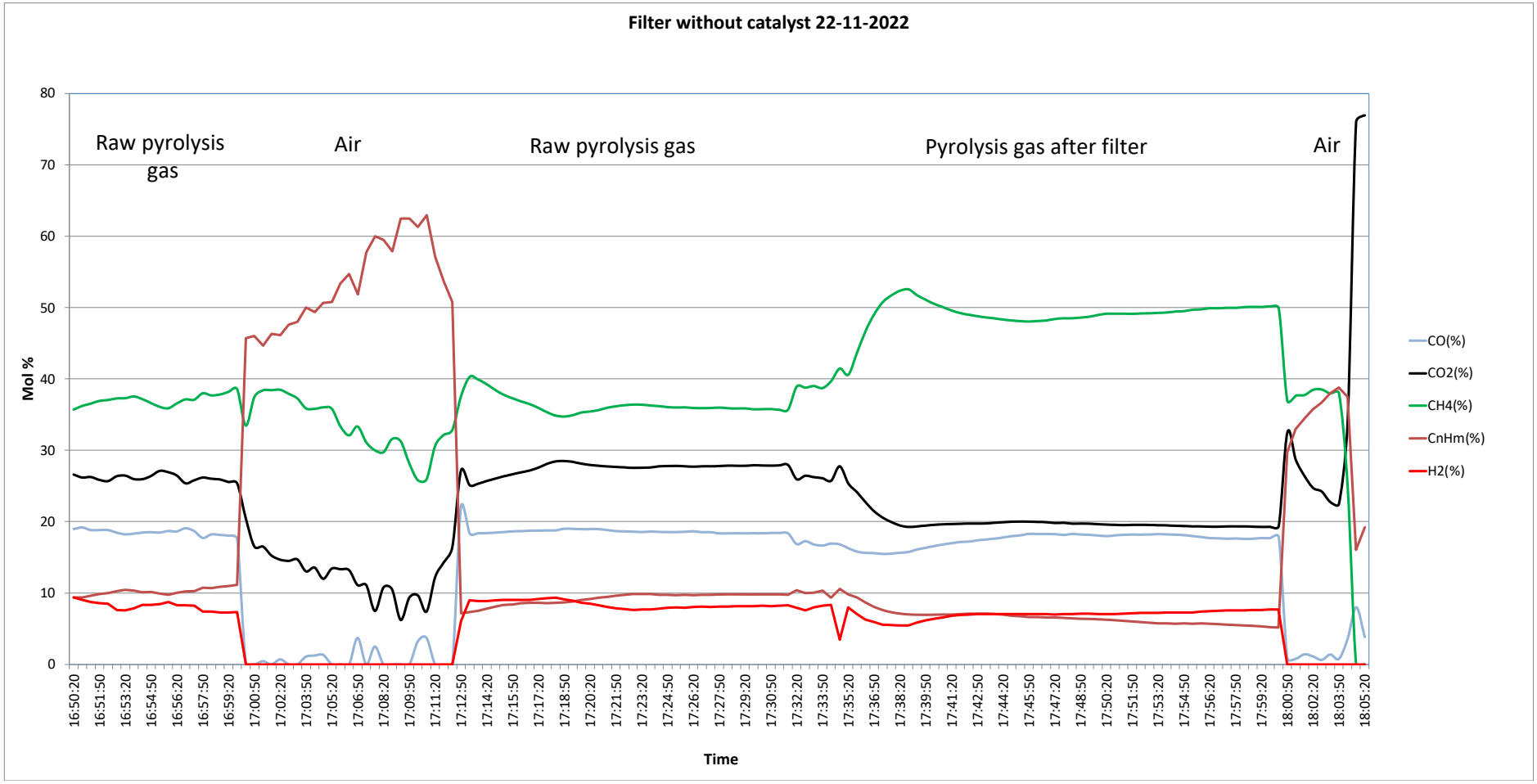

Figure 9 Composition of non-condensable gas components, excluding N_2 and O_2, over time during the candle filter test November 22 measured with a Hubei Cubic-Ruiyi 3100P gas analyzer.

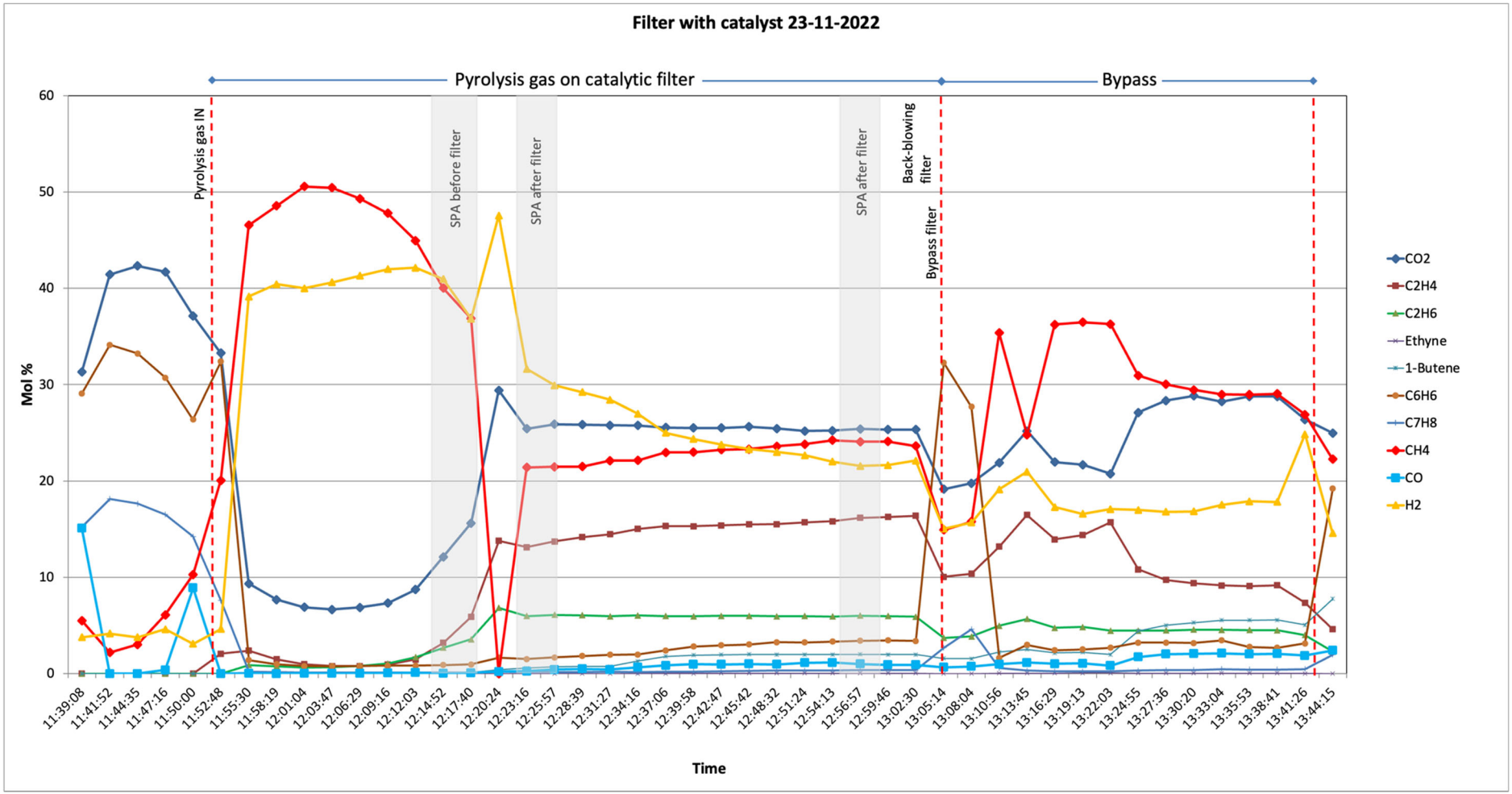

Figure 10 Composition of non-condensable gas components over time during the catalytic filter test November 23 measured with the μ-GC. The gas content is shown as oxygen and nitrogen free.

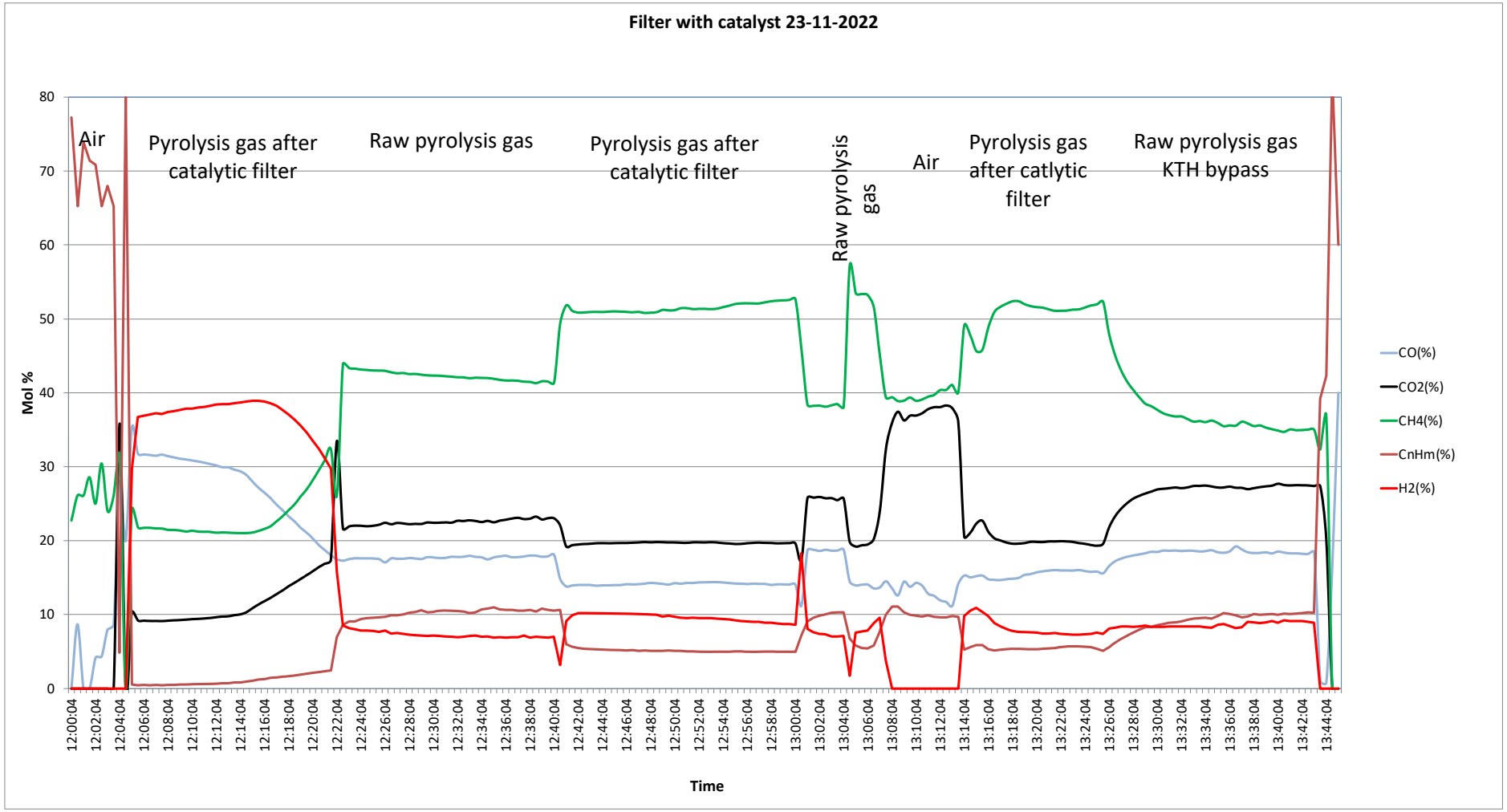

Figure 11 Composition of non-condensable gas components, excluding N_2 and O_2, over time during the catalytic filter test November 23 with a Hubei Cubic-Ruiyi 3100P gas analyzer.

4.3. Ash in residues

Table 6 shows the ash content of char and fly ash samples collected from the two test runs. Assuming a major part of the removed during the oxidation of the sample is carbon, the residual streams roughly contain on average 50 % of C. Neglecting other solid residues in the gas stream, the not converted C roughly corresponds to 35 % of the C in the fed RDF.

Since the amount of collected filter ash from the back blowing of the filter was rather low no analysis could be performed on this sample using the described method.

Table 6 Summary of ash content in solid samples

Test date	November 22, 2022	November 23, 2022
Ash in char after pyrolyzer (wt%)	57.2	58.1
Ash in fly ash cyclone (wt%)	46.0	46.0

4.4. Condensable organic compounds

Amounts of condensable organic compounds detected using the filter and catalytic filter the raw pyrolysis gas is shown in Table 7. The original amounts are given in the unit (µg/100 ml) as based on the sample volume collected during the tests. Recalculation of the values to gram condensable organic compounds per kilogram waste feed and is presented in Table 8. Also, carbon content in tar is calculated, using benzene as an average condensable organic compound, and shown in the table. The basis for this is the negligible amounts of phenols (in the order of 10-20 µg/100 ml) present in the samples and the amount of benzene present in the samples. The content of condensable organics is higher after the filter, or the catalytic filter, compared to samples collected before for all cases. Note the large increase in naphthalene, which is larger compared than the increase of BTX (benzene, toluene, xylene) and sum of aromatics.

The amount detectable condensable organics are high (Table 8), even though the method only considers aromatics and phenols below a molecular weight of X and X g/mol, respectively.

Table 7 Summary of the chemical analysis of condensable organic compounds as determined in the 100 ml gas sample (µg/100 ml). (BTX: benzene, toluene, xylene)

	November 22, 2022	November 22, 2022	November 23, 2022	November 23, 2022	November 23, 2022
	SPA before filter 16:12 -->	SPA after filter 16:25 -->	SPA before filter 12:16 -->	SPA after filter 12:22 -->	SPA after filter 12:55 -->
Component	Quantity [µg/100 ml]	Quantity [µg/100 ml]	Quantity [µg/100 ml]	Quantity [µg/100 ml]	Quantity [µg/100 ml]
Total BTX	3522	8686	7966	9271	11015
Naphthalene	124	930	440	1078	1269
Total > Naphthalene	253	798	648	801	1596
Sum Aromatics [µg/100ml]	4004	10869	9419	11450	14350

Table 8 Condensable organic compounds recalculated to corresponding to produced gas volume and per kg RDF

		µg tar/100 ml dry gas	g tar/Nm3	g tar/kg fuel	g C in tar/Nm3	g C in tar/kg fuel
Test 2022-11-22	Before	4024	40	101	37	93
	After	10889	109	272	100	251
Test 2022-11-23	Before	9439	94	236	87	218
	After	12920	129	323	119	298

4.5. Carbon balance

A carbon balance can be estimated from the total carbon in the gas and residual carbon in the char and fly ash (Table 6). Other information needed for calculation is collected from sources as detailed in Appendix 1. Estimated rough carbon balances are presented in Table 9.

Table 9 Summary of roughly estimated carbon balances

	22-11-2022	23-11-2022
% C in permanent gases	58.4	62.5
% C in condensable organics	4.4	10.9
% C permanent gases + condensable organics	**62.8**	**73.4**

5. Discussion

The results of the changes in gas composition for the gas passing through the catalytic filter clearly shows it is catalytically active as shown in Figure 10 and Figure 11. A clear correlation between H_2 and CH_4, mirroring each other, is observed, indicating a potential decomposition of methane to hydrogen or another decomposition process of hydrocarbon(s) linked to H_2 and CH_4. However, methane is the most difficult to decompose catalytically and the temperature of 750 °C used in the present tests are a bit too low for decomposing methane. In general, the decomposition occurs most easily for the largest organics with increasing difficulty the lighter the hydrocarbons become. In the present case, this is to a large extent also true for benzene and naphthalene, important intermediates in a decomposition scheme (Figure 3). Methane formed probably originates from fragments of larger molecules or from methylene groups bonded to aromatics.

The observed change in content of condensable organics (Table 7 and Table 8)may at first sight point at an increasing content of condensable organics. However, the SPA method only analyzes part of the condensable organics, leaving a larger part of hydrocarbons undetected. This is also apparent from the carbon balance (Table 9) missing a major part of the carbon in the pyrolysis vapors, including a fraction of heavier hydrocarbons. Therefore, the observed larger amount of tar for non-condensable organics after the pyrolysis vapors passing the catalytic filter, should be seen as a result from decomposition of heavier hydrocarbons. For example, the increase in naphthalene is 2.5 times compared to the increase in sum of aromatics of 1.2 of after the catalytic filter. This shows that heavier condensable organics not detected by SPA ends up as naphthalene, a rather stable molecule difficult to decompose catalytically at the temperature used in the tests. In future tests, a different pyrolysis vapor sampling method should be used, such as a train of impinger bottles with different liquids for absorbing the different types of non-condensable organics.

Also, the results from the test using only filter shows a certain degree of decomposition of the heavier condensable organics, as indicated by the the slow increase in CH_4 and H_2, simultaneously as the decrease of C_nH_m in time (17:43 – 18:00) as shown in Figure 9. Since the other gas compounds are constant during the same period, the buildup of a filter cake, decomposing some of the C_nH_m could be a re reason for the observed change. However, decomposition of other components cannot be excluded although this would most likely change the composition of the other non-condensable gases. Nevertheless, as for the catalytic filter, a larger content of condensable organics is detected with a 7.5 time increase of naphthalene compared to only a 2.7 time increase for the sum of aromatics (Table 7) when the gas is passing through the filter. This shows that the decomposition ends up in naphthalene to larger extent than in case of the catalytic filter, where catalytic processes are in play.

The carbon balances, including permanent and condensable gas compounds, for the two tests count only for 60 (22-11-2022) and 70 % (23-11-2023) of the estimated carbon available in the produced gas. This is partly due to the limitations in the SPA analysis method. There is however a large uncertainty in the estimated gas flow and an increase of 20-30 % in gas flow would increase estimated C to 70-80 and 80-90% for the two cases. The C not identified in the carbon balance is certainly heavier condensable hydrocarbons not detected by the SPA method. To account for these hydrocarbons a parallel gravimetric sampling of the gas should have been performed. This is something to consider in parallel with SPA sampling in future potential test campaigns.

The catalytic activity of the filter only lasts for appr. 20-25 minutes which of course is an unacceptable time in view of commercial application. The reason for the short active time is most likely carbon formation on the surface, is a well-known cause of deactivation on Ni catalyst surfaces[7]. A rapid deactivation due to carbon formation is very likely due to the very low content of water vapor (10%) in the pyrolysis vapors. Generally, a higher content is needed to slow down the carbon formation, but exact amount is not easy to assess and depends on gas composition and the catalyst temperature. A temperature above 800 °C is preferred, but even higher up to 900°C is better, and a water vapor content of 20-30 % would have been preferred. In a commercial application, the catalytic filter will also be regenerated using high temperature steam removing the carbon from the surface. Additionally, almost certainly also a lower flow per surface area of catalyst in a series of filter elements should be used to prolong the time of catalytic activity. A series of elements facilitates a simultaneous filtration catalytic conversion and regeneration of deactivated catalyst surfaces.

Since the application aims at using the gas in a gas engine for power production with there is no need to completely decompose the condensable organics ($\leq$50mg/Nm^3 for > C_5 hydrocarbons). A catalytic filter or catalytic reactor using iron-based catalytic materials[8,9] would probably be a better choice since it is less sensitive for sulfur impurities and is cheaper. Iron-based catalyst have a good performance in catalytic decomposition of tars in gasification processes[8] and also been applied in pyrolysis processes for gas conditioning[9].

6. Conclusions

The weather conditions were not ideal with heavy rain and rather low temperatures for the instrument used and in view of the conditions, the experiments were carried out successfully with a rather smooth operation of the filter test rig. Below are the main findings and conclusions listed:

- The formation of methane in the catalytic filter test shows that larger organic compounds are decomposed by the catalyst.
- The filter also displayed a certain reduction in heavier hydrocarbons.
- The catalytic filter was only active for a short time of 20-25 minutes, which is probably due to a low water content in the gas. Another explanation could also be exposure to pyrolysis vapor with a too high content of organics.

[7] Bartholomew CH. Mechanisms of catalyst deactivation. Appl Catal A: Gen 2001;212:17–60.
[8] V. Nemanova, T. Nordgreen, K. Engvall, K. Sjöström, Biomass gasification in an atmospheric fluidised bed: Tar reduction with experimental iron-based granules from Höganäs AB, Sweden, Catalysis Today, 176 (1) (2011) 253-257.
[9] P. H. Mouda, E. Kantarelis, K. J. Andersson, K. Engvall, Biomass pyrolysis gas conditioning over an iron-based catalyst for mild deoxygenation and hydrogen production, Fuel, 211 (2018) 149–158

- Regeneration with steam is important in future industrial applications.
- For the application in mind utilizing the gas in a gas engine, a Ni based catalyst is probably not the best choice. An iron-based material could be a feasible alternative.
- A lower flow per surface area of catalyst in a series of filter elements should be used to prolong the time of catalytic activity.

Looking into the rear-view mirror, it would have wise to have a pre-visit on site at 3B to better understand the process, need for information and the conditions for performing the test campaigns. The following activities or conditions should be included in future test campaigns:

- To account for these hydrocarbons a parallel gravimetric sampling of the gas should have been performed in parallel with SPA sampling.
- An improved gas conditioning equipment before gas analysis
- More filter elements, both catalytic and non-catalytic

Appendix 1 Gas analysis with the Hubei Cubic-Ruiyi 3100P gas analyzer including N_2 and H_2.

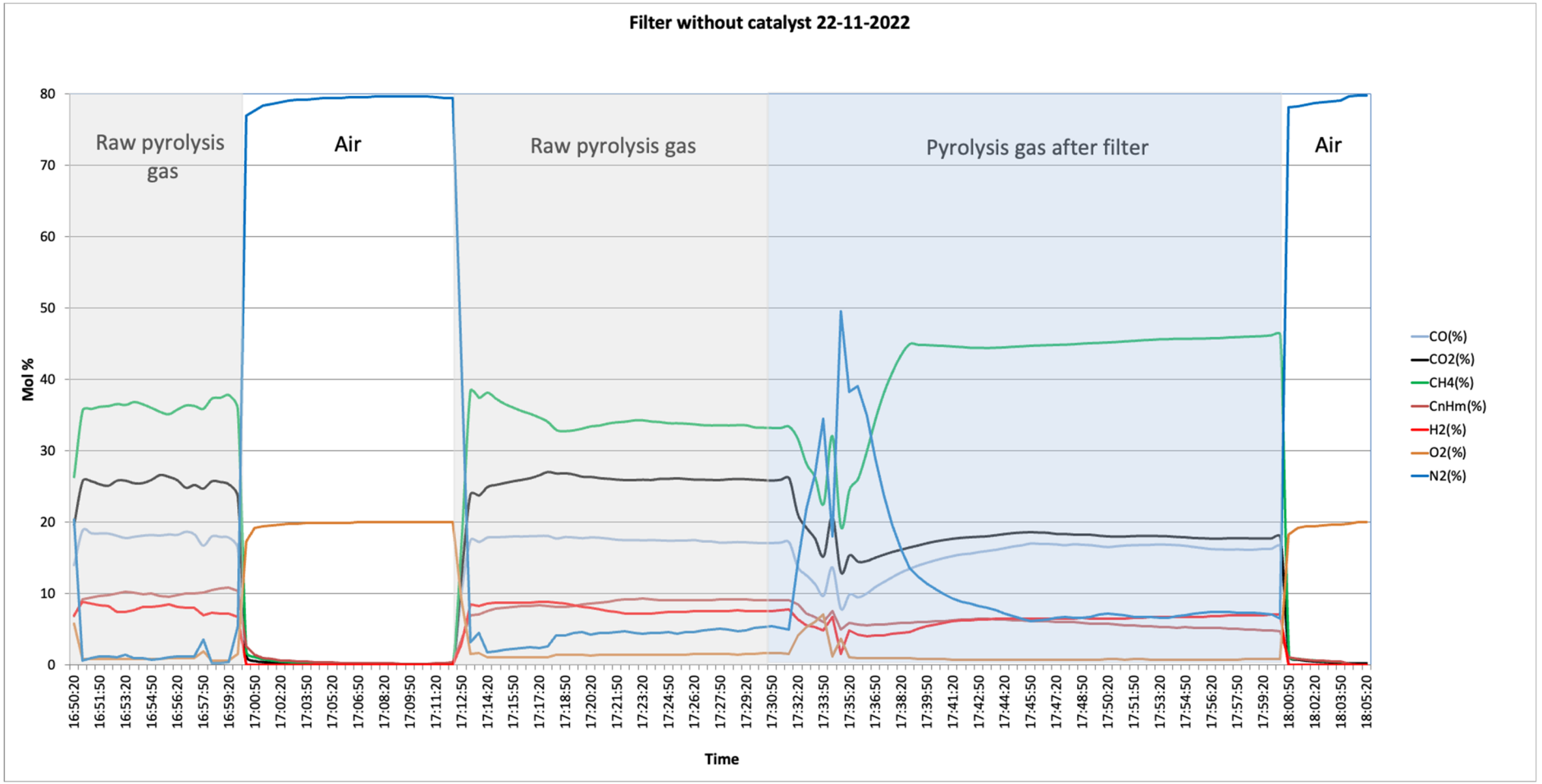

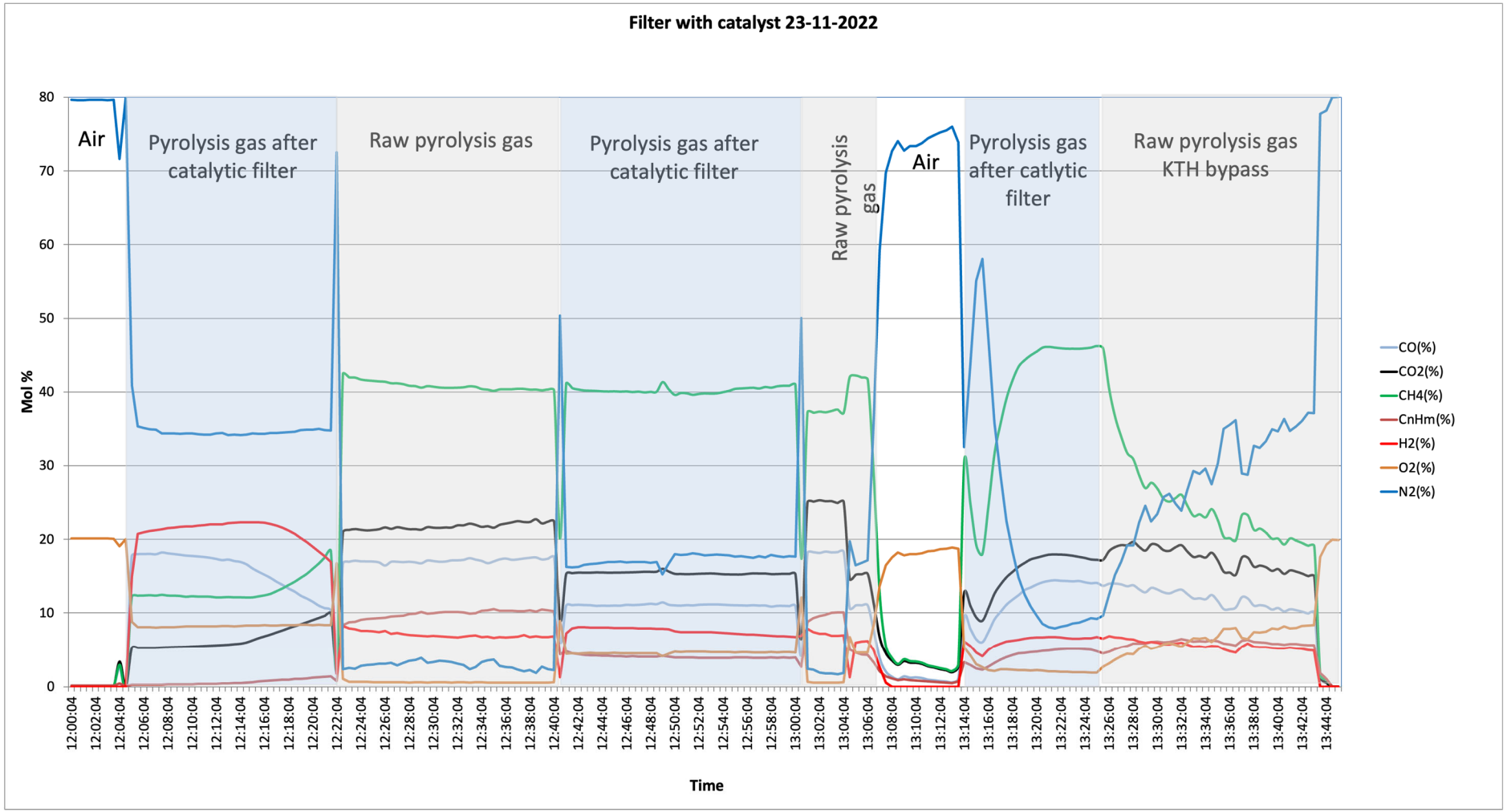
Filter with catalyst 23-11-2022
Air
Pyrolysis gas after catalytic filter
Raw pyrolysis gas
Pyrolysis gas after catalytic filter
Raw pyrolysis gas
Air
Pyrolysis gas after catlytic filter
Raw pyrolysis gas KTH bypass
Mol %
Time
CO(%)
CO2(%)
CH4(%)
CnHm(%)
H2(%)
O2(%)
N2(%)

Appendix 2 Carbon balance

Data				2022-11-22	2022-11-23								
Waste fed	25	kg dry		88	93								
Gas produced	10	Nm3/h dry gas		35,2	37,2								
Humidity	10	%											
2022-11-22													
Gas composition	vol %	vol %	V (m3)	Vtotalt (m3)	Vtotalt (m3)	g C 22/11	Molviktförhål	Molvikten					
CO	17,2	18,4	0,45	6,48	6,85	2953,28	0,42857143	26				V=nRT/P	
CO2	25,9	27,8	0,68	9,76	10,32	4789,17	0,27272727	44					
CH4	33,6	36,0	0,88	12,66	13,38	6212,97	0,75	16				101300	P
CnHm (C2)	9,2	9,9	0,24	3,47	3,66	3402,34	0,85714286	28				298	T
H2	7,5	8,0	0,20	2,83	2,99							8,314	R
O2	1,6	0,0	0,00	0	0,00								
N2	5,1	0,0	0,00	0	0,00							n=PV/RT	
	100,1	100,1	2,45	35,2	37,20	17357,76							
65% C in gas													
2022-11-23													
Gas composition	vol %	vol %	V (m3)	Vtotalt (m3)	Vtotalt (m3)	g C 23/11	Molviktförhål	Molvikten					
CO	17,2	17,8	0,44	6,27	6,63	3021,04	0,42857143	26					
CO2	21,9	22,7	0,56	7,99	8,44	4142,44	0,27272727	44					
CH4	40,6	42,1	1,03	14,81	15,65	7679,60	0,75	16					
CnHm (C2)	9,9	10,3	0,25	3,61	3,82	3745,22	0,85714286	28					
H2	6,7	7,0	0,17	2,44	2,58								
O2	0,6	0,0	0,00	0	0,00								
N2	3	0,0	0,00	0	0,00								
	99,9	99,9	2,44	35,1296703	37,13	18588,30							
Totalt C in gas	29,744	kg/h											
	22-nov	23-nov											
% C i permanenta gaser	**58,4**	**62,5**											
% C in oil vapours	**4,40**	**10,90**											
% C perm gas + oil	**62,8**	**73,4**											
Test 2022-11-22	Before	4024	µg tar/100 ml dry gas		40,24	g tar/Nm3	100,6	g tar/kg fuel	37,1446154	g C in tar/Nm3	92,8615385	g C in tar/kg fuel	
	After	10889	µg tar/100 ml dry gas		108,89	g tar/Nm3	272,225	g tar/kg fuel	100,513846	g C in tar/Nm3	251,284615	g C in tar/kg fuel	
Test 2022-11-23	Before	9439	µg tar/100 ml dry gas		94,39	g tar/Nm3	235,975	g tar/kg fuel	87,1292308	g C in tar/Nm3	217,823077	g C in tar/kg fuel	
	After	12920	µg tar/100 ml dry gas		129,2	g tar/Nm3	323	g tar/kg fuel	119,261538	g C in tar/Nm3	298,153846	g C in tar/kg fuel	